IL NUOVO CIMENTO Vol. 24 C, N. 3 Maggio-Giugno 2001

Stability analysis of solid particle motion in rotational flows(*)

P. Paradisi(1) and F. Tampieri(2)

(1) *Dipartimento di Ingegneria Energetica, Nucleare e del Controllo Ambientale Università di Bologna - Viale Risorgimento 2, I-40136 Bologna, Italy*

(2) *ISAO-CNR - via Gobetti 101, I-40129 Bologna, Italy*

(ricevuto il 27 Ottobre 2000; approvato il 26 Febbraio)

Summary. — A two-dimensional model of a rotational flow field is used to perform the stability analysis of solid particle motion. It results that the stagnation points are equilibrium points for the motion of particles and the stability analysis allows to estimate their role in the general features of particle motion and to identify different regimes of motion. Furthermore, the effects of Basset history force on the motion of particles lighter than the fluid (*bubbles*) are evaluated by means of a comparison with the analytical results found in the case of Stokes drag. Specifically, in the case of bubbles, the vortex centres are stable (attractive) points, so the motion is dominated by the stability properties of these points. A typical convergence time scale towards the vortex centre is defined and studied as a function of the Stokes number St and the density ratio γ. The convergence time scale shows a minimum (nearly, in the range $0.1 < St < 1$), in the case either with or without the Basset term. In the considered range of parameters, the Basset force modifies the convergence time scale without altering the qualitative features of the particle trajectory. In particular, a systematic shift of the minimum convergence time scale toward the inviscid region is noted. For particles denser than the fluid, there are no stable points. In this case, the stability analysis is extended to the vortex vertices. It results that the qualitative features of motion depend on the stability of both the centres and the vertices of the vortices. In particular, the different regimes of motion (diffusive or ballistic) are related to the stability properties of the vortex vertices. The criterion found in this way is in agreement with the results of previous authors (see, *e.g.*, Wang *et al.* (*Phys. Fluids*, **4** (1992) 1789)).

PACS 92.60.Mt – Particles and aerosols.
PACS 47.55.Kf – Multiphase and particle-laden flows.
PACS 47.55.Dz – Drops and bubbles.

(*) The authors of this paper have agreed to not receive the proofs for correction.

1. – Introduction

The motion of particles in non-uniform rotational viscous flows has received attention by many authors, because of the variety of effects displayed in different conditions. Despite the interest on this topic, the role of the Basset history force did not receive much attention, due to the lack of analitycal methods and to the time-consuming numerical schemes necessary for the integration of the Basset term, which is represented by an integral of the past accelerations weighted by an algebraic function.

We will address the problem of a single small rigid sphere, thus neglecting shape deformation and interaction among particles. The literature is fairly extensive and we shall review quite shortly some relevant results. As far the law of motion is concerned, the viscous non-uniform flow problem was addressed by Maxey and Riley [1], and non-zero Reynolds number effects on the drag were summarized by Soo [2] and Clift *et al.* [3]. Special attention to unsteady effects (Basset force) was given by Lovalenti and Brady [4-7] and Mei and Adrian [8] among others. Shear in the flow induces lift, as discussed by Saffman [9], McLaughlin [10] and Mei [11] for the case of linear shear in viscous flow and by Auton *et al.* [12] in the generic inviscid rotational case.

The features of the particle motion in periodic cellular flow in two or three dimensions (basically, ABC flow) were investigated by Crisanti *et al.* [13], Maxey and Corrsin [14], Wang *et al.* [15], McLaughlin [16], considering different approximations for the law of motion, in particular, neglecting acceleration effects (Basset term) and lift force. Tio *et al.* [17] studied the motion in periodic Stuart vortices, accounting for the (inviscid) lift. More complex flow fields derived from DNS—Elgobashi and Truesdell [18], Ling *et al.* [19]—have been investigated. Notice that because of the approximations involved in the motion law, some of these studies concern limited ranges of particle density.

In this work we are interested in the qualitative evaluation of the changes induced by memory effects, *i.e.* by the Basset hystory force, in a rotational flow. For this reason, we shall limit to a simple analytical model, representing a periodic steady flow field, described by the streamfunction (see Townsend [20], pp. 7-9 for details)

$$\psi = UL\cos(x/L)\cos(y/L)\,. \tag{1}$$

The flow field is periodic in both directions, being constituted by a sequence of identical vortices (see fig. 1). For this flow field and for fixed Stokes number St (given by the ratio between the Stokes time scale and the flow time scale: see later for a quantitative definition) Crisanti *et al.* [13] observed that particles lighter than the fluid (*bubbles*) are captured in the vortex centres, whereas particles denser than the fluid present chaotic behaviour for particle-to-fluid density ratio

$$\gamma = \rho_{\mathrm{P}}/\rho_{\mathrm{F}} \tag{2}$$

not much greater than 1 (say, $1 < \gamma < 1.4$) and ballistic behaviour for denser particles. Wang *et al.* [15] observed that the particle behaviour also changes as the Stokes number changes. This means that the inertia of the particle has to become large enough with respect to drag in order to allow the particle trajectory to be chaotic.

Here we shall evaluate the order of magnitude of the Basset force and its effect on the motion of bubbles around a vortex centre. The motion law will be introduced in sect. **2**, the stability properties of the vortex centres will be analyzed in sect. **3**. In sect. **4** a convergence time scale for light particles will be introduced and the effects of Basset

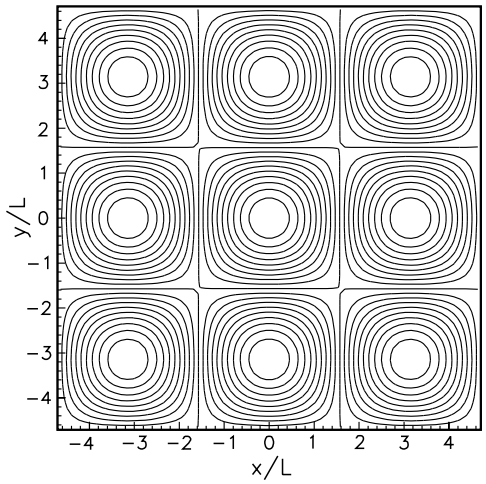

Fig. 1. – Pattern of the two-dimensional flow field.

force will be studied. Section **5** is dedicated to the stability properties of vortex vertices and their relations with the qualitative behaviour of dense particles. In sect. **6** some conclusions are drawn.

2. – The equation of motion

The particle motion is considered here as the result of inertial and drag force effects. Any external force will be neglected, as well forces deriving from density gradients [21]. Also the lift force will be neglected. Thus, the equation of motion is

$$m_{\mathrm{P}} \frac{\mathrm{d}\mathbf{v}}{\mathrm{d}t} = \mathbf{F}_{\mathrm{i}} + \mathbf{F}_{\mathrm{d}} \,, \tag{3}$$

where m_{P} is the particle mass and $\mathbf{v}$ its velocity. $\mathbf{F}_{\mathrm{i}}$ represents the sum of the forces related to the inertia of both the particle and the surrounding fluid (*i.e.* the inviscid terms) and $\mathbf{F}_{\mathrm{d}}$ the drag force, related to the fluid viscosity. According to Auton *et al.* [12] and to Sene *et al.* [22] the pressure gradient and added mass forces read

$$\mathbf{F}_{\mathrm{i}} = m_{\mathrm{F}} \left[(1 + C_M) \frac{\mathrm{D}\mathbf{u}}{\mathrm{D}t} - C_M \frac{\mathrm{d}\mathbf{v}}{\mathrm{d}t} \right] , \tag{4}$$

where $\mathbf{u}$ is the flow velocity, m_{F} is the mass of the volume of fluid displaced by the impurity, *i.e.* $m_{\mathrm{F}} = m_{\mathrm{P}}/\gamma$, C_M is the added mass coefficient. The derivative along the fluid motion

$$\frac{D}{\mathrm{D}t} = \frac{\partial}{\partial t} + \mathbf{u} \cdot \nabla \tag{5}$$

is used, whereas $\mathrm{d}/\mathrm{d}t$ represents the derivative along the solid particle motion. The added mass coefficient C_M is taken to be equal to 1/2.

In the limit of negligibly small particle Reynolds number given by

$$Re_p = \frac{a \mid \mathbf{v} - \mathbf{u} \mid}{\nu} \quad , \tag{6}$$

ν being the kinematic viscosity of the fluid and a the particle radius, the drag force is expressed as the sum of the Stokes (steady) force and the Basset (unsteady) force:

$$\mathbf{F}_{\mathrm{d}} = -6\pi a\mu \left[\mathbf{v} - \mathbf{u} + a \int_{t_0}^{t} \frac{\mathrm{d}(\mathbf{v} - \mathbf{u})/\mathrm{d}\tau}{\sqrt{\nu\pi(t-\tau)}} \mathrm{d}\tau \right] \tag{7}$$

according to Maxey and Riley [1]. Here $\mu = \rho_{\mathrm{F}}\nu$ is the dynamic viscosity of the fluid. It is worth noting that for small but nonzero Reynolds number the above formula has to be considered as a first approximation, strictly valid for short times, of the order of the viscous time scale

$$T_* = \frac{a^2}{\nu} \, . \tag{8}$$

Lovalenti and Brady [4-7] show as more complex expressions can be written, accurate to $O(Re)$: according to the Oseen correction to the Stokes formula, the decay turns out to be faster than Basset's $t^{-1/2}$. However these effects have not been investigated here, our main purpose being the qualitative evaluation of the changes induced by memory effects.

Note that together with $Re_p \ll 1$ the Stokes drag law holds (Maxey and Riley [1]) if $T_*/\Theta \ll 1$, which means that the diffusive time scale is much smaller than the eddy overturning time scale Θ defined as $\Theta = L/U$. A further limitation related to pressure gradient and added mass effects is $a/L \ll 1$, *i.e.* the size of the particle must be small enough to assume constant pressure gradient on its surface [1].

Let us now define the relaxation time of the particle, or Stokes time scale T:

$$T = \frac{m_I + C_M m_F}{6\pi a\mu} = \frac{2}{9} T_* (\gamma + C_M) \tag{9}$$

and note that the Basset term may be conveniently written in terms of fractional derivative of order 1/2 (see Caputo [23] and Caputo and Mainardi [24]):

$$D_*^{1/2} f(t) = \frac{1}{\Gamma(1/2)} \int_0^t \frac{\mathrm{d}f(\tau)/\mathrm{d}\tau}{\sqrt{t-\tau}} \mathrm{d}\tau \, . \tag{10}$$

The equation of motion is made nondimensional by normalizing the variables on the flow scales U, L and $\Theta = L/U$:

$$\frac{\mathrm{d}\mathbf{v}}{\mathrm{d}t} = A \frac{\mathrm{D}\mathbf{u}}{\mathrm{D}t} - \frac{1}{St} \left[(\mathbf{v} - \mathbf{u}) + Ba^{1/2} D_*^{1/2} (\mathbf{v} - \mathbf{u}) \right] , \tag{11}$$

$$A = \frac{1 + C_M}{\gamma + C_M} \quad ; \quad St = \frac{T}{\Theta} \quad ; \quad Ba = \frac{T_*}{\Theta} \, . \tag{12}$$

For sake of simplicity the nondimensional variables are still indicated with the same notation as before and, in the next sections, we agree to consider only nondimensional

quantities. Henceforth, we refer to eq. (11) without the Basset term ($Ba = 0$) as the *Stokes approximation*.

A comparison with the work by Crisanti *et al.* [13] shows that their equation of motion can be derived from eq. (11) with $C_M = 0$, and neglecting the Basset term. Thus their Stokes time scale is given by eq. (9) with $C_M = 0$. In the limit of very dense particles their expression is thus equivalent to the present one, whereas deviations are expected for light bubbles.

At variance with the choice made in this paper (namely eq. (4)), Wang *et al.* [15] used the following expression for the pressure gradient and added mass forces:

$$\mathbf{F}_i = m_{\text{F}} \left[\frac{\mathrm{D}\mathbf{u}}{\mathrm{D}t} + C_M \frac{\mathrm{d}\mathbf{u}}{\mathrm{d}t} - C_M \frac{\mathrm{d}\mathbf{v}}{\mathrm{d}t} \right] \tag{13}$$

and neglected the Basset force. The previous expression allows to distinguish between the mass of the fluid displaced by the particle, which accelerates according to the fluid motion, and the mass of fluid carried with the particle, which accelerates according to the particle motion. This point may deserve further investigations; however comparing our results with Wang's ones it seems that no relevant differences appear in the considered parameter range.

3. – Stability analysis of vortex centres

It is recognized that in the cellular flow field the centres and the vertices of the cells are equilibrium points, whose stability has been discussed by Crisanti *et al.* [13], Maxey [25], Wang *et al.* [15] in the case of the simplified equation of motion.

It results in particular that vortex centres are attractive points for particles less dense than the fluid, *i.e.* for bubbles. Tio *et al.* [17] investigated the stability of the equation with the lift included, for the periodic Stuart vortex flow. We shall present here a similar analysis for our flow field, referring to eq. (11). This extends the analysis by Wang *et al.* [15] and gives a basis for a comparison with Basset force effects, in the range of application of the present formulation.

Linearizing around the vortex centre $(x_1; x_2) = (0; 0)$, the solution for the equation of motion (11) without the Basset term is expressed for each component x_i of the particle position vector $\mathbf{x}$ as a linear combination of decaying exponentials: $x_i \sim \sum_k \exp[-\lambda_k t]$; the values of λ_k are obtained by a fourth-order eigenvalue equation and are function of the relative density γ and of the Stokes number St. The eigenvalue equation reads

$$\lambda^4 + C_3\lambda^3 + C_2\lambda^2 + C_1\lambda + C_0 = 0\,, \tag{14}$$

where

$$C_3 = -\frac{2}{St}\,, \tag{15}$$

$$C_2 = \frac{1}{St^2} + 2\ A\,, \tag{16}$$

$$C_1 = -\frac{2\ A}{St}\,, \tag{17}$$

$$C_0 = \frac{1}{St^2} + A^2\,. \tag{18}$$

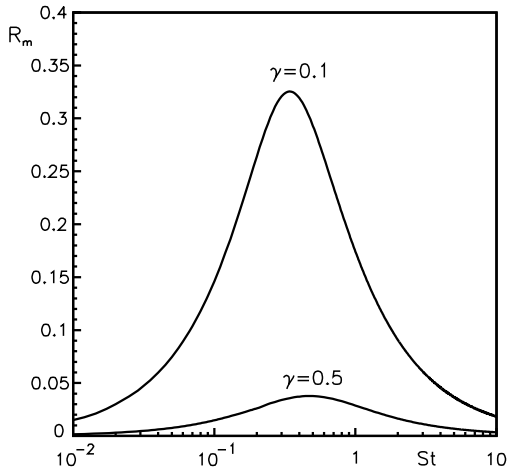

Fig. 2. – Real parts of the eigenvalue $\mathcal{R}_m$ in the vortex centre.

Note that being the time t measured in unit of Θ, the eigenvalues are in units of $\omega_\Theta = 1/\Theta$ (this is the frequency of fluid particle motion in the neighborhood of the vortex centre).

The eigenvalues in the vortex centre are complex conjugates; it results that the first two eigenvalues have always a positive real part, whereas the other two have:

– positive real part if $\gamma < 1$ (asymptotically stable equilibrium),

– zero if $\gamma = 1$ (stable),

– negative if $\gamma > 1$ (unstable).

In every case the second couple of eigenvalues has the smaller absolute real part $\mathcal{R}_m$. In the first case the particles are attracted by the vortex centre and the second couple of eigenvalues defines the time needed to the light particle to converge towards the centre, whereas in the unstable case the same eigenvalue gives an estimate of the growth rate of the distance of the particle from the vortex centre.

The real parts of each eigenvalue are given by the following expression:

$$\mathcal{R}_\pm = \frac{1}{2St} \pm \frac{1}{\sqrt{2}St} F(St, A)\,, \tag{19}$$

$$F = \left\{ \frac{1}{4} - ASt^2 + \left[\left(\frac{1}{4} - ASt^2 \right)^2 + St^2 \right]^{1/2} \right\}^{1/2} . \tag{20}$$

In this case $\mathcal{R}_m$ is given by the minus sign in eq. (19). Note that similar expressions have been obtained by other authors (see, for example, [25]). In fig. 2 $\mathcal{R}_m$ is reported as a function of St for $\gamma = 0.5$ and $\gamma = 0.1$. in the case $\gamma > 1$ the qualitative behaviour of $\mathcal{R}_m$ is similar to the case $\gamma < 1$, but with negative values. This can be seen in fig. 3 ($\gamma = 1.26$).

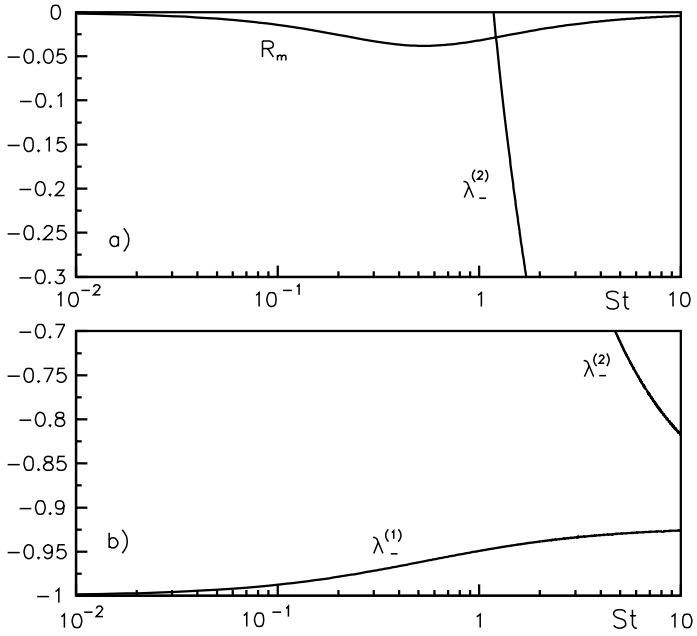

Fig. 3. – Comparison between the real parts of the eigenvalues in the centre and in the vertices, for particles denser than the surrounding fluid ($\gamma = 1.26$). $\lambda_-^{(2)}$ becomes negative for $St > 1/A$, whereas $\lambda_-^{(1)}$ and $\mathcal{R}_m$ are always negative.

4. – Motion of bubbles and convergence times

The motion of bubbles (*i.e.* $\gamma < 1$) is dominated by the stability properties of the vortex centres. The time necessary to reach the centre is measured by the convergence time scale

$$T_{\mathrm{c}} = \mid \mathcal{R}_m \mid^{-1} \quad . \tag{21}$$

T_{c} can also be estimated from numerically computed trajectories fitting the distance r of the particle from the vortex centre with an exponential function: $r(t) \sim \exp[(-t/T_{\mathrm{c}})]$. The numerical estimation agrees well with the analytical one (in the Stokes approximation).

The convergence time scale T_{c}, computed from eqs. (19) and (21) (*i.e.* neglecting the Basset term), is plotted as a function of St in fig. 4 for different values of the parameter γ. First, T_{c} shows a minimum for $0.1 < St < 1$ and the value of the minimum is a function of the density ratio γ. Note that the convergence time T_{c} increases with the density ratio (for fixed St).

Both for vanishing viscosity and for very large viscosity the convergence time diverges; for $\nu \to 0$ it results $St \to \infty$ and

$$T_{\mathrm{c}} \simeq 2 \frac{A^{1/2}}{A^{1/2} - 1} \; St\,; \tag{22}$$

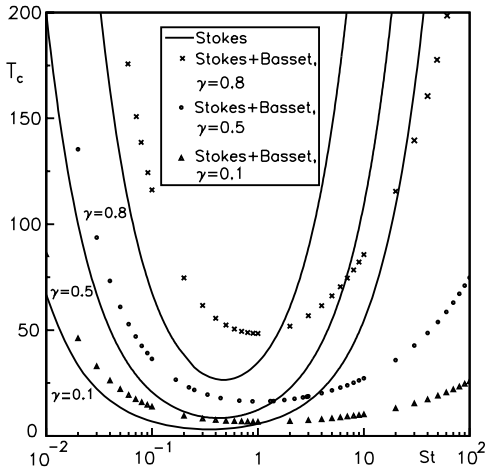

Fig. 4. – Comparison of convergence time scales for different values of the relative density γ and different formulation of the motion law. The pressure gradient and added mass terms are always included.

the asymptotic behaviour for $\nu \to \infty$ ($St \to 0$) is

$$T_c \simeq \frac{1}{(A-1)\ St}\,. \tag{23}$$

This analysis is clearly valid under the condition $\gamma \neq 1$; for $\gamma = 1$ the particle always move along a streamline for every value of St, so that T_c is infinite ($\mathcal{R}_m = 0$).

By summarizing the analysis of the simplified equation which accounts for pressure gradient, added mass and Stokes drag, it appears that the light particles converge towards the vortex centre for any finite St, but the time scale for convergence becomes very large in the case of large viscosity (because particles are trapped on a streamline and follow the fluid motion, after a transient depending on the initial conditions) and in the case of negligible viscosity (because the particles move along closed trajectories different from streamlines, without dissipation). Qualitatively the effect may be appreciated looking at fig. 5, where trajectories computed for particles with $\gamma = 0.5$ and for different values of St are reported. Clearly, the actual time needed to converge towards the centre depends on the initial conditions: if the particle is far from the centre or has an initial velocity different from that of the fluid, a transient occurs before the trajectory takes the form of a spiral.

Some sample trajectories and the convergence times have been computed also in the complete case (Basset term included). The numerical integration has been performed using a forward Euler scheme (suitable for the computation of trajectories in the convergence case) with a product-integration scheme to represent the fractional derivative (see Mainardi *et al.* [26]). The slow algebraic decay of the memory term forces the integration to be performed using a large number of terms describing the past accelerations: in practice no one was neglected for the integration up to 100 (*i.e.* for 10^5 time steps). The convergence time scale has been estimated by means of an exponential fit of the distance $r(t)$ between the particle and the vortex center. In the neighbourhood of the vortex centre (say for $r(t) = |\mathbf{x}| < 0.1$) the behaviour of $r(t)$ is accurately represented

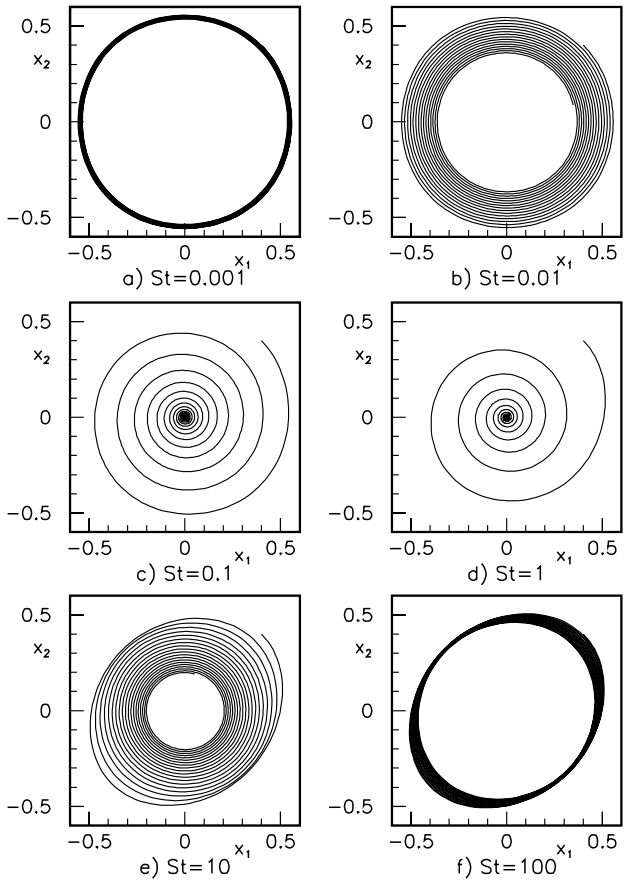

Fig. 5. – Sample trajectories for particles lighter than the surrounding fluid ($\gamma = 0.5$) without the effect of Basset term. The trajectories are computed for the same time interval (up to 100 in units of Θ) and with the same initial conditions: $\mathbf{x}_0 = (0.4, 0.4)$ and $\mathbf{v}(t = 0) = \mathbf{u}(\mathbf{x}_0)$.

by a decaying exponential $r(t) \simeq r(0) \exp[-t/T_c]$ (see fig. 6). The values obtained in selected cases are reported in fig. 4. The overall effect is to shift the minimum position rightwards (towards the inviscid regime), and to change the shape of the curve in such a way to enhance the effect of viscous drag (*i.e.* considering the same fluid viscosity ν, the presence of Basset term increases the viscous drag with respect to the case with the Stokes drag only).

5. – Stability analysis of vortex vertices and behaviour of dense particles

As discussed in sect. **3**, the vortex centre is an unstable point for dense particles ($\gamma > 1$). In order to study the features of particle trajectories, it is necessary to perform a stability analysis of the vortex vertices. This stability analysis has been performed for the cell vertices $(x_1; x_2) = (\pm\pi/2; \pm\pi/2)$ for eq. (11) without the Basset term. The

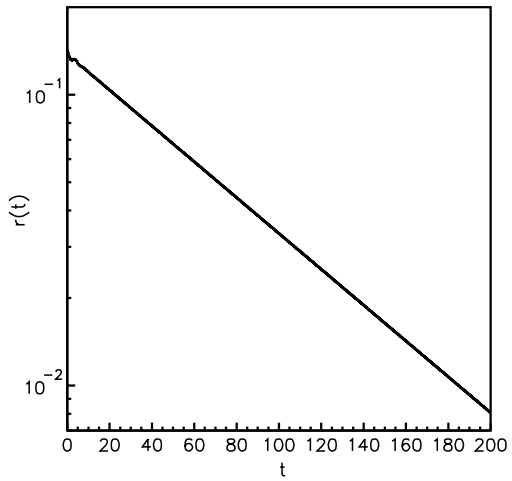

Fig. 6. – The distance $r(t)$ of the particle by the vortex centre shows an exponential decay also with the Basset term included. Here we have $\gamma = 0.8$, $St = 6$.

corresponding eigenvalue equation (the same for each vertex) reads

$$\left[\lambda\left(\lambda + \frac{1}{St}\right) - A_1\right]\left[\lambda\left(\lambda + \frac{1}{St}\right) - A_2\right] = 0\,, \tag{24}$$

$$A_1 = A - \frac{1}{St}\,, \tag{25}$$

$$A_2 = A + \frac{1}{St}\,, \tag{26}$$

where A is given by eq. (12). Note that $A < 1$ for $\gamma > 1$.

The solutions of the eigenvalues equation are given by the following expressions:

$$\lambda_{\pm}^{(1)} = \frac{1}{2\ St}\left\{1 \pm \left[4A\ St^2 + 4\ St + 1\right]^{1/2}\right\}, \tag{27}$$

$$\lambda_{\pm}^{(2)} = \frac{1}{2\ St}\left\{1 \pm \left[4A\ St^2 - 4\ St + 1\right]^{1/2}\right\}. \tag{28}$$

The first two eigenvalues, $\lambda_{\pm}^{(1)}$, are always real and distinct. $\lambda_{-}^{(1)}$ is strictly less than zero for all values of γ and St, so all these points are unstable. The two others, $\lambda_{\pm}^{(2)}$, are complex conjugate with positive real part for

$$\frac{(1 - \sqrt{1 - A})}{2A} \leq St \leq \frac{(1 + \sqrt{1 - A})}{2A} \quad ; \quad \gamma > 1\,. \tag{29}$$

Outside this range they become real; $\lambda_{+}^{(2)}$ remains always positive, whereas $\lambda_{-}^{(2)}$ can be either positive or negative. It results that the directions of the eigenvectors are contained

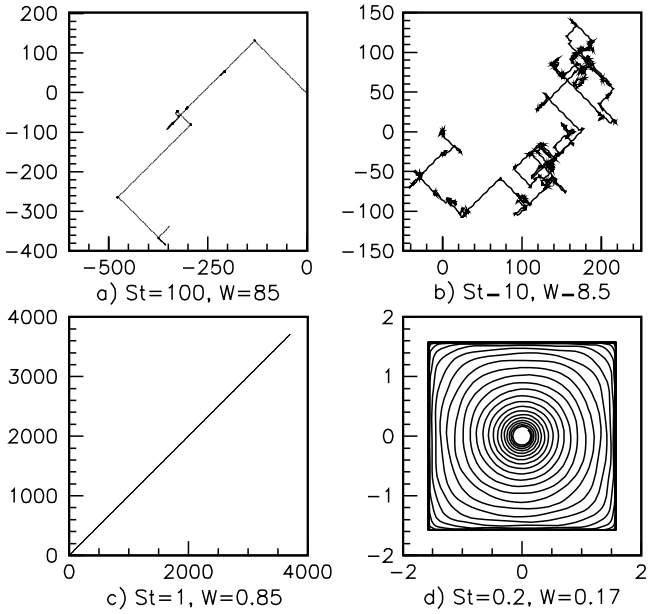

Fig. 7. – Sample trajectories for particles denser than the surrounding fluid without the effect of Basset term ($\gamma = 1.26$). The trajectories are computed up to 10000 (in units of Θ) with initial conditions: $\mathbf{x}(0) = (0.1; 0.1)$ and $\mathbf{v}(0) = \mathbf{u}(\mathbf{x}(0))$.

in the phase planes (x_1, v_1) and (x_2, v_2) (separately for $\lambda_{\pm}^{(1)}$ and $\lambda_{\pm}^{(2)}$), so that in the plane (x_1, x_2) these directions are along the separatrices. The direction of $\lambda_{\pm}^{(1)}$, along the separatrix, is always repulsive, whereas the stability of the other direction depends by the sign of $\lambda_{-}^{(2)}$. In fig. 3 the (negative) real part of the eigenvalues for $\gamma = 1.26$ are reported for both the centre ($\mathcal{R}_m$) and the vertices ($\lambda_{-}^{(1)}$ and $\lambda_{-}^{(2)}$) as functions of St. It can be seen that $\lambda_{-}^{(1)}$ remain always negative while $\lambda_{-}^{(2)}$ becomes negative for $St > 1/A$, adding a second unstable direction (along the other separatrix) in the neighbourhood of the vertices. Thus, both the directions become unstable for

$$W = St\ A > 1\,. \tag{30}$$

The aymptotic values of $\mathcal{R}_m$ are zero for both the limits $St \to 0$ and $St \to \infty$; $\lambda_{-}^{(1)}$ tends to -1 as $St \to 0$ and to $-A^{1/2}$ as $St \to \infty$; this last limit is the same also for $\lambda_{-}^{(2)}$.

Let us now consider the qualitative behaviour of dense particles in the light of the previous discussions, looking at sample trajectories, displayed in fig. 7, numerically evaluated for different values of the parameters. In fig. 7 the effect of increasing viscosity (decreasing St) is enlighted. In the range $St > 10$ (see figs. 7 (a)-(b)) the particles show an average motion along directions $\mid x \mid = \mid y \mid$ (*i.e.* parallel to the diagonal of the cells); depending on the value of St they turn out to be captured by a vortex (rarely in the example of fig. 7 (a), more often in case (b)). After some time they leave the vortex in a new unpredictable direction. We also observe that, in the range $St > 1$, the time spent along a fixed direction is longer for greater St. With reference to the previous analysis,

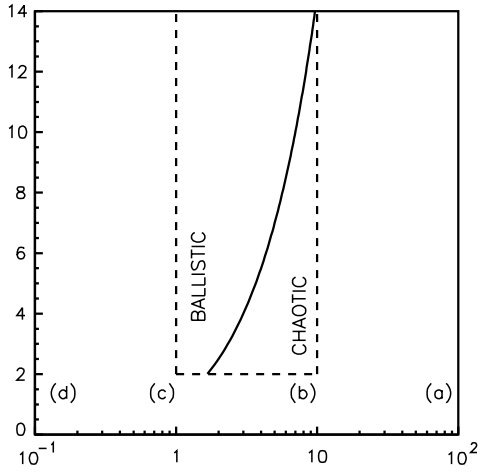

Fig. 8. – Parameter space (St, γ). The dashed line defines the region studied by Wang *et al.* Letters identify the cases reported in fig. 7.

we note that $W > 1$ in cases (a) and (b). Figure 7 (c) shows a typical ballistic behaviour, namely $\langle x^2 \rangle \sim t^2$, for $St = 1$ and $W < 1$. For large viscosity ($St < 1$, $W < 1$) the particle tends to spend long time on the separatrices (see fig. 7 (d)) and in particular near the crossings after the initial transient is finished (due for instance to an initial velocity different from that of the fluid or to a initial position near the vortex centre). These features appear to be consistent with the change of sign of the eigenvalue ($\lambda_-^{(2)}$) in the crossing points. This happens for $St > 1/A$, *i.e.* $W > 1$.

Similar results were obtained by Wang *et al.* [15]. They investigated the range $1 < St < 10$ and $\gamma > 2$ and found that the behaviour of dense particles depends by the ratio between the pressure gradient force and the Stokes drag. In particular, when the pressure gradient force is dominant, the particle behaviour is diffusive ($\langle x^2 \rangle \sim t$, compare with fig. 7 (a-b)), otherwise ballistic behaviour is observed (fig. 7 (c)). In our notation, the Wang criterion for diffusive regime is given by

$$St \, \frac{\alpha}{2(\gamma + C_M)} > 1 \,, \tag{31}$$

where the value of α is evaluated to be 2 or 3 dependent on which choice we made about the inertia expression (eq. (13) or eq. (4), respectively): we choose $\alpha = 3$. In both the cases, the essence of the results is the same. The Wang relation (31) expresses the same relationship between St and γ given by our stability analysis, eq. (30). Figure 8 shows, in the $(St; \gamma)$-plane, the domains of chaotic (diffusive) and ballistic behaviour according to Wang *et al.* [15]. The letters (a), (b), (c) locate the cases examined previously and displayed in fig. 7, which show properties consistent with Wang *et al.* analysis. Note that the results obtained by Crisanti *et al.* [13] are consistent with those obtained by Wang *et al.* [15]. They considered the case with $T = 1$ and $\Theta = 1/2$ (namely, $St = 2$) and stated that for $1 < \gamma < 1.4$ diffusive behaviour occurs, while, for larger γ values, the position variance grows ballistically.

A further observation is in order, considering the case of fig. 7 (d), which should display a ballistic behaviour, according to the value of W. Numerical experiments for

small St put into evidence that an impurity with initial position near to the vortex centre takes a longer time to leave the vortex itself with respect to an impurity starting near the separatrix. The time necessary to leave the cell (a sort of *escape time*) increases as St decreases, according to the behaviour of the eigenvalue with the smallest absolute value of the real part (see $\mathcal{R}_m$ in fig. 3).

6. – Conclusions

For the case of particles lighter than the surrounding fluid, the stability analysis of the solid particles motion around the vortex centers of a periodic flow field has been numerically performed taking into account the Basset hystory force. The convergence time of the particle has been compared with the analitycal expression obtained in the Stokes approximation. It has been shown that the Basset force acts as a further drag without altering the qualitative features of the particle trajectory, increasing the convergence time for large viscosity ($St < 1$) and decreasing it in the small viscosity range ($St > 1$).

For the case of dense particles, we limited ourselves to study the stability in the simplified case (without Basset term). The transition from chaotic (diffusive) to ballistic behaviour, already studied by Wang *et al.* [15], has been justified looking at the stability properties of vortex vertices. From the analysis of the numerical simulations, it results that, in the ballistic regime with $St < 1$, the escape time from the initial vortex appears to increase as St decreases. This effect may hinder the ballistic behaviour for short simulation times.

* * *

This work was partially supported by the INTAS-RFBR 95-723 Project "Two-phase turbulence in hydrodynamics, cosmology and nonlinear acoustics".

REFERENCES

[1] Maxey M. R. and Riley J. J., *Phys. Fluids*, **26** (1983) 883.
[2] Soo S. L., *Fluid Dynamics of Multiphase Systems* (Blaisdell Publishing Company, London) 1967.
[3] Clift R., Grace J. R. and Weber M. E., *Bubbles, Drops and Particles* (Academic, New York) 1978.
[4] Lovalenti P. M. and Brady J. F., *J. Fluid Mech.*, **256** (1993) 561.
[5] Lovalenti P. M. and Brady J. F., *J. Fluid Mech.*, **256** (1993) 607.
[6] Lovalenti P. M. and Brady J. F., *Phys. Fluids A*, **5** (1993) 2104.
[7] Lovalenti P. M. and Brady J. F., *J. Fluid Mech.*, **293** (1995) 35.
[8] Mei R. and Adrian R. J., *J. Fluid Mech.*, **237** (1992) 323.
[9] Saffman P. G., *J. Fluid Mech.*, **22** (1965) 385; also see *Corrigendum*, **31** (1968), p. 624.
[10] McLaughlin J. B., *J. Fluid Mech.*, **224** (1991) 261.
[11] Mei R., *Int. J. Multiphase flow*, **18** (1992) 145.
[12] Auton T. R., Hunt J. C. R. and Prud'homme M., *J. Fluid Mech.*, **197** (1988) 241.
[13] Crisanti A., Falcioni M., Provenzale A. and Vulpiani A., *Phys. Lett. A*, **150** (1990) 79.
[14] Maxey M. R. and Corrsin S., *J. Atmos. Sci.*, **43** (1986) 1112.
[15] Wang L. P., Maxey M. R., Burton T. D. and Stock D. E., *Phys. Fluids A*, **4** (1992) 1789.
[16] McLaughlin J. B., *Phys. Fluids*, **31** (1988) 2544.

[17] Tio K. K., Gañán-Calvo A. M. and Lasheras J. C., *Phys. Fluids*, **5** (1993) 1679.
[18] Elgobashi S. and Truesdell G. C., *J. Fluid Mech.*, **242** (1992) 655.
[19] Ling W., Chung J. N., Troutt T. R. and Crowe C. T., *J. Fluid Mech.*, **358** (1998) 61.
[20] Townsend A. A., *The Structure of Turbulent Shear Flow*, 2 edition (Cambridge University Press, Cambridge) 1976.
[21] Eames I. and Hunt J. C. R., *J. Fluid Mech.*, **353** (1997) 331.
[22] Sene K. J., Hunt J. C. R. and Thomas N. H., *J. Fluid Mech.*, **259** (1994) 219.
[23] Caputo M., *Geophys. J. R. Astron. Soc.*, **13** (1967) 529.
[24] Caputo M. and Mainardi F., *Pure Appl. Geophys.*, **91** (1971) 134.
[25] Maxey M. R., *Phys. Fluids*, **30** (1987) 1915.
[26] Mainardi F., Pironi P. and Tampieri F., *A numerical approach to the generalized Basset problem for a sphere accelerating in a viscous fluid*, in *Proceedings of 3rd Annual Conference of the CFD Society of Canada - CFD 95, Banff, Alberta, Canada: June 25-27, 1995*, edited by Thibault P. A. and Bergeron D. M., Vol. **2**, pp. 105-112.